

Ionic and Poly(ionic liquids) as Perovskite Passivating Molecules for Improved Solar Cell Performances

Silvia Mariotti,^a Daniele Mantione,^a Samy Almosni,^b Milutin Ivanović,^a Takeru Bessho,^b Miwako Furue,^b Hiroshi Segawa,^{b*} Georges Hadziioannou,^a Eric Cloutet,^{a*} Thierry Toupance.*

Affiliations

^a Univ. Bordeaux, CNRS, Bordeaux INP, LCPO, UMR 5629, Allée Geoffroy Saint-Hilaire, B8, F-33615 Pessac, Cedex, France.

^b Research Center for Advanced Science and Technology (RCAST), The University of Tokyo, Komaba Research Campus, 4 Chome-6-1 Komaba, Meguro City, Tokyo 153-0041, Japan.

^c Univ. Bordeaux, CNRS, Bordeaux INP, ISM, UMR 5255, 351 Cours de la Libération, F-33405 Talence, Cédex, France.

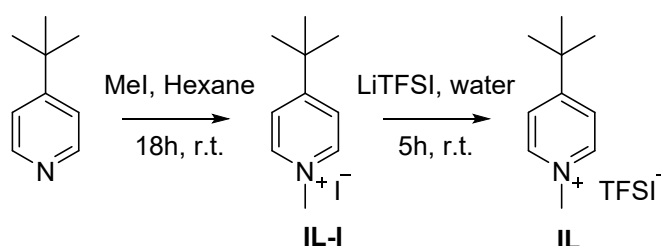
Supporting Information Content Sections:

1.	Materials and methods	1
2.	IL Synthesis and NMR data	1
3.	PIL synthesis and NMR data	2
4.	Solar cell preparation	10
5.	Solar cell characterisation	10

1. Materials and Methods

Deuterated solvent and NMR tubes were bought from Eurisotop. Iodomethane was bought from TCI. Lithium bistrifluoromethanesulfonimide (Li-TFSI) was bought from Acros Organics. Poly(4-vinylpyridines) average $M_w \approx 60,000$ and $12,000 \text{ g.mol}^{-1}$ were bought from Sigma Aldrich. Dry solvents were bought from Acros Organics (AcroSeal Packaging) and used without further purification. All other chemicals were supplied from Fisher Scientific. NMR spectra were recorded at $25 \text{ }^\circ\text{C}$ with a 400 MHz Bruker Avance. Data are reported in chemical shift (ppm), multiplicity (s, singlet; d, doublet; q, quartet; the signals are referenced to the residual solvent DMSO- d_6 ($\delta = 2.50 \text{ ppm } ^1\text{H}$, $39.520 \text{ ppm } ^{13}\text{C}$) or CDCl_3 ($\delta = 7.26 \text{ ppm } ^1\text{H}$, $77.160 \text{ ppm } ^{13}\text{C}$).

2. IL Synthesis and NMR data

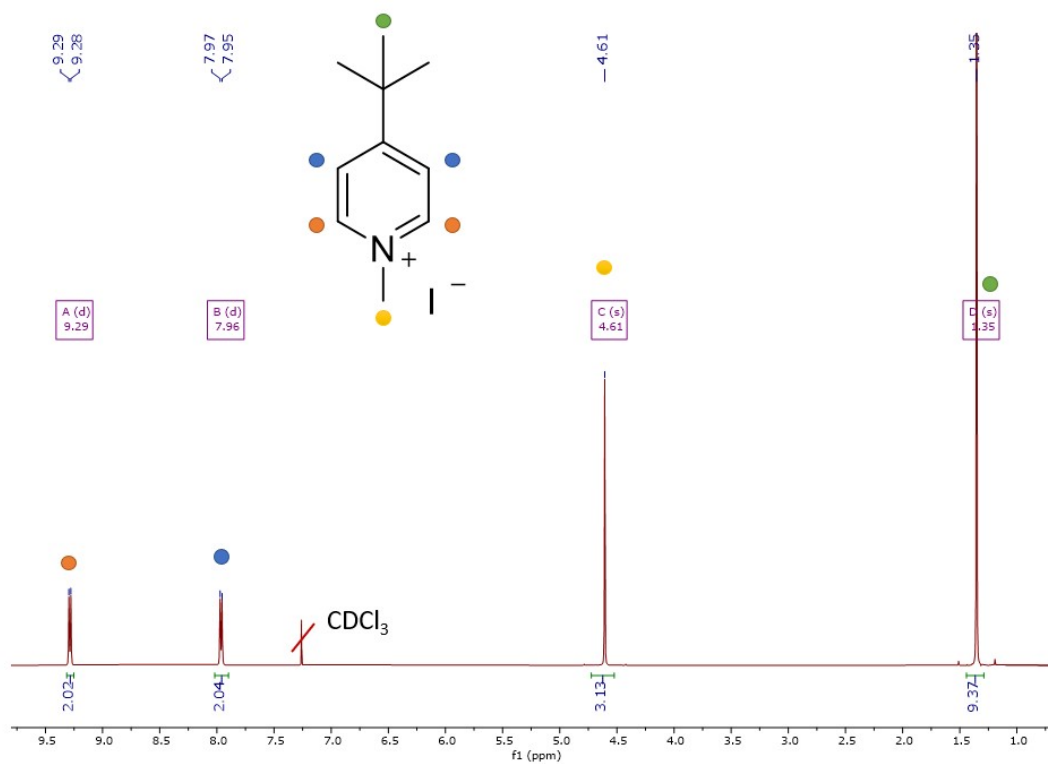


Scheme S1. Synthetic route towards IL-I and IL

4-(tert-butyl)-1-methylpyridinium iodide IL-I

In a 100 mL round bottom flask, 1g (7.4 mmol) of 4-tertbutyl pyridine was dissolved in 10 mL of dry hexane. An excess of Iodomethane 4 mL (9.12 g, 64 mmol) was added to this solution. The solution immediately turned turbid and the mixture was stirred for 18 more hours in order to ensure the completion and then it was quickly filtered. The yellow precipitate was washed three times with 20 mL dry hexane and dried under vacuum for 24 h. Yield 1.78 g (87 m.p. $143\text{-}145 \text{ }^\circ\text{C}$, FT-IR ν_{max} [cm^{-1}]: 3073 =C-H , $2235 \text{ C}\equiv\text{N}$, 1612 -C=C- , $1408 \text{ -CH}_2\text{- scissoring}$, $950 \text{ aromatic bending}$, 655 bending =C-H .

^1H NMR (400 MHz, CDCl_3) δ 9.29 (d, $J = 7.0$ Hz, 2H), 7.96 (d, $J = 7.1$ Hz, 2H), 4.61 (s, 3H), 1.35 (s, 9H). ^{13}C NMR (101 MHz, CDCl_3) δ 170.93, 145.10, 125.27, 48.44, 36.65, 30.04.



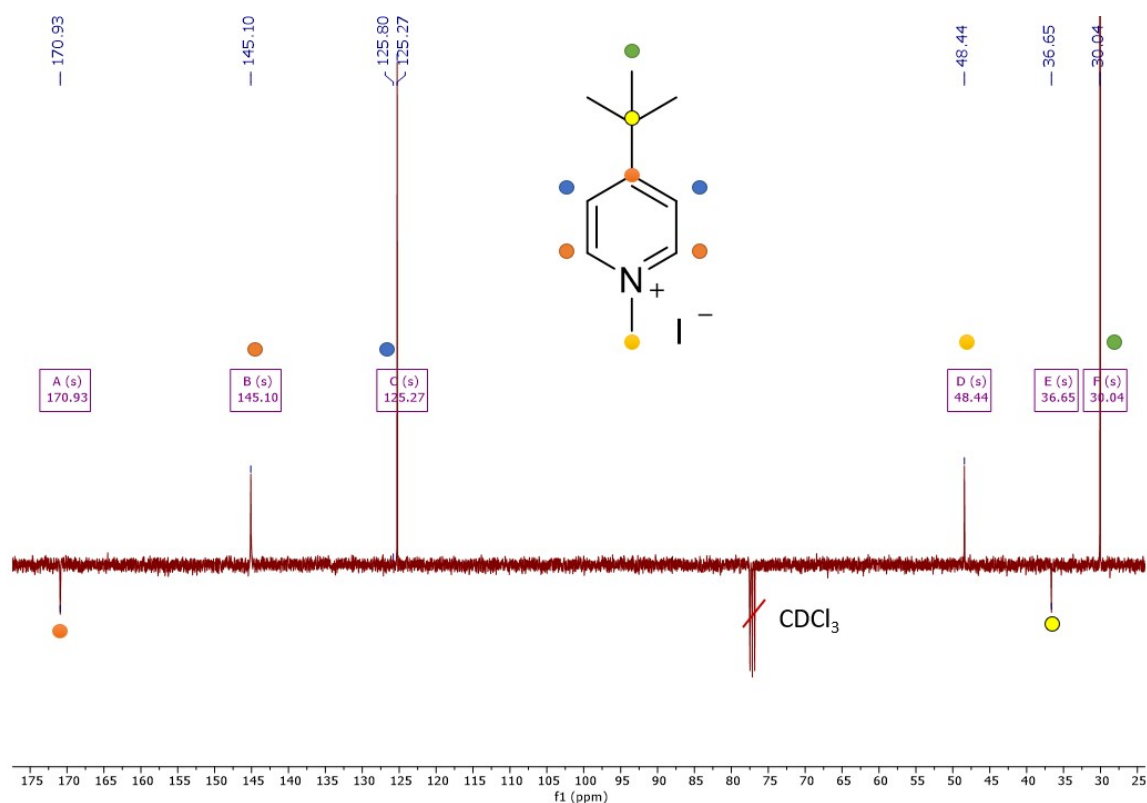


Figure S2. ^{13}C NMR APT spectrum of **IL-I** in CDCl_3

4-(tert-butyl)-1-methylpyridinium bistrifluoromethanesulfonimide **IL**

In a 50 mL beaker equipped with a magnetic stirrer, 0.5g (1.8 mmol) of 4-(tert-butyl)-1-methylpyridinium iodide (**IL-I**) was dissolved in 20 mL of DI water. An excess of four times of Li-TFSI 2.07 g (7.2 mmol) was added to this solution. The solution immediately turned turbid and the mixture was stirred for 5 more hours in order to ensure the completion and then it was filtered. The white precipitate was washed three times with 20 mL water and dried under vacuum for 24 h. Yield 0.77 g (ca. 100%); m.p. 186-189 °C, FT-IR ν_{max} [cm^{-1}]: 3073 =C-H, 2235 $\text{C}\equiv\text{N}$, 1612 -C=C-, 1408 - CH_2 - scissoring, 1250 - CF_3 , 1102 - SO_2 -, 950 aromatic bending, 750 scissoring CF_3 , 655 bending =C-H.

^1H NMR (400 MHz, CDCl_3) δ 8.15 (d, J = 7.0 Hz, 2H), 7.47 (d, J = 7.0 Hz, 2H), 3.87 (s, 3H), 0.95 (d, J = 1.4 Hz, 9H). ^{13}C NMR (101 MHz, CDCl_3) δ 171.36, 144.45, 125.33, 119.74 (q, J = 321.3 Hz), 47.57, 36.53, 29.74. ^{19}F NMR (377 MHz, DMSO-d_6) δ -81.14.

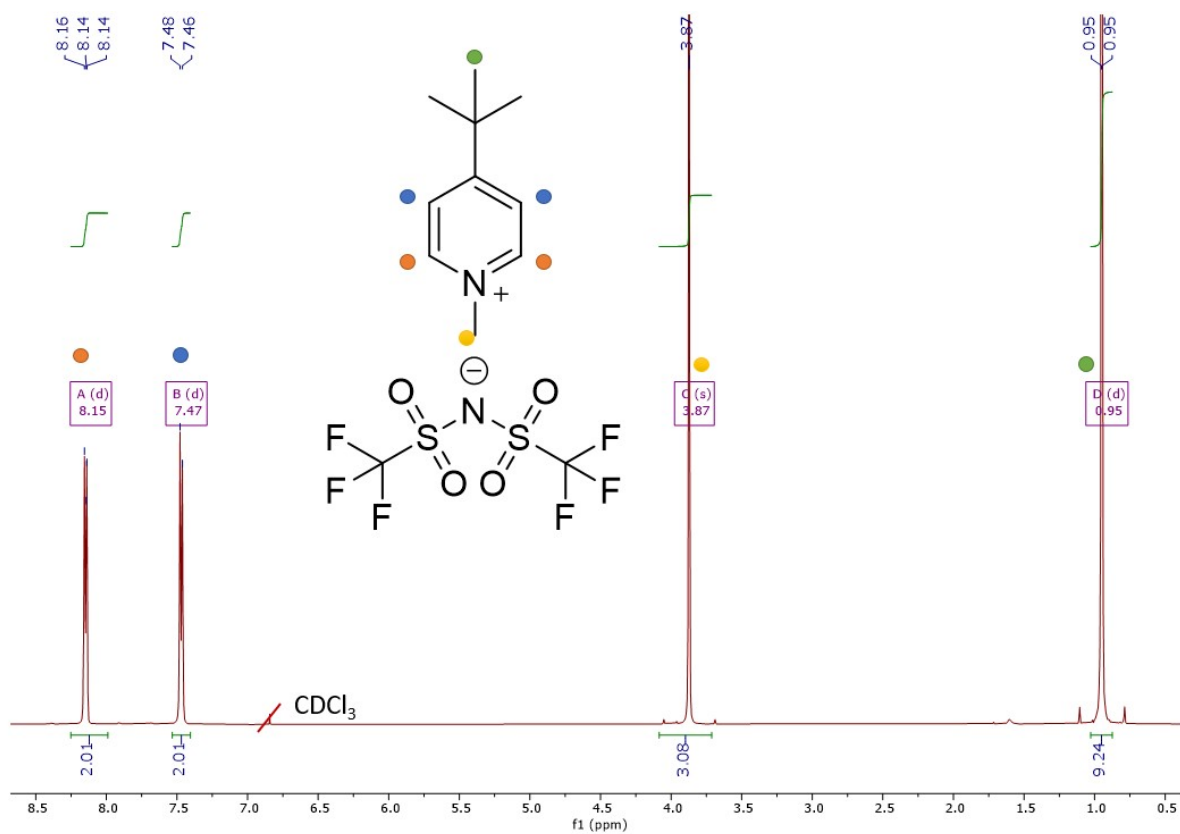


Figure S3. ^1H NMR spectrum of **IL** in CDCl_3

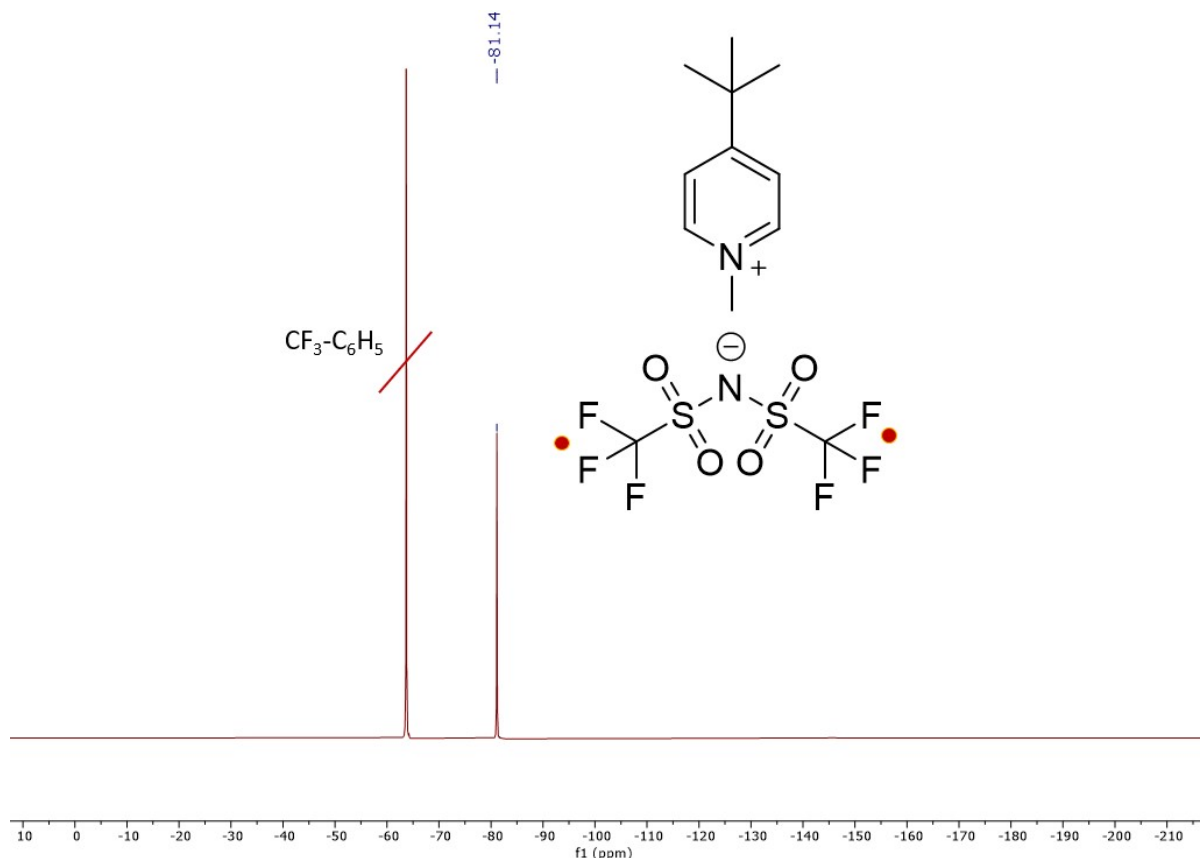


Figure S4. ^{19}F NMR spectrum of **IL** in DMSO-d_6

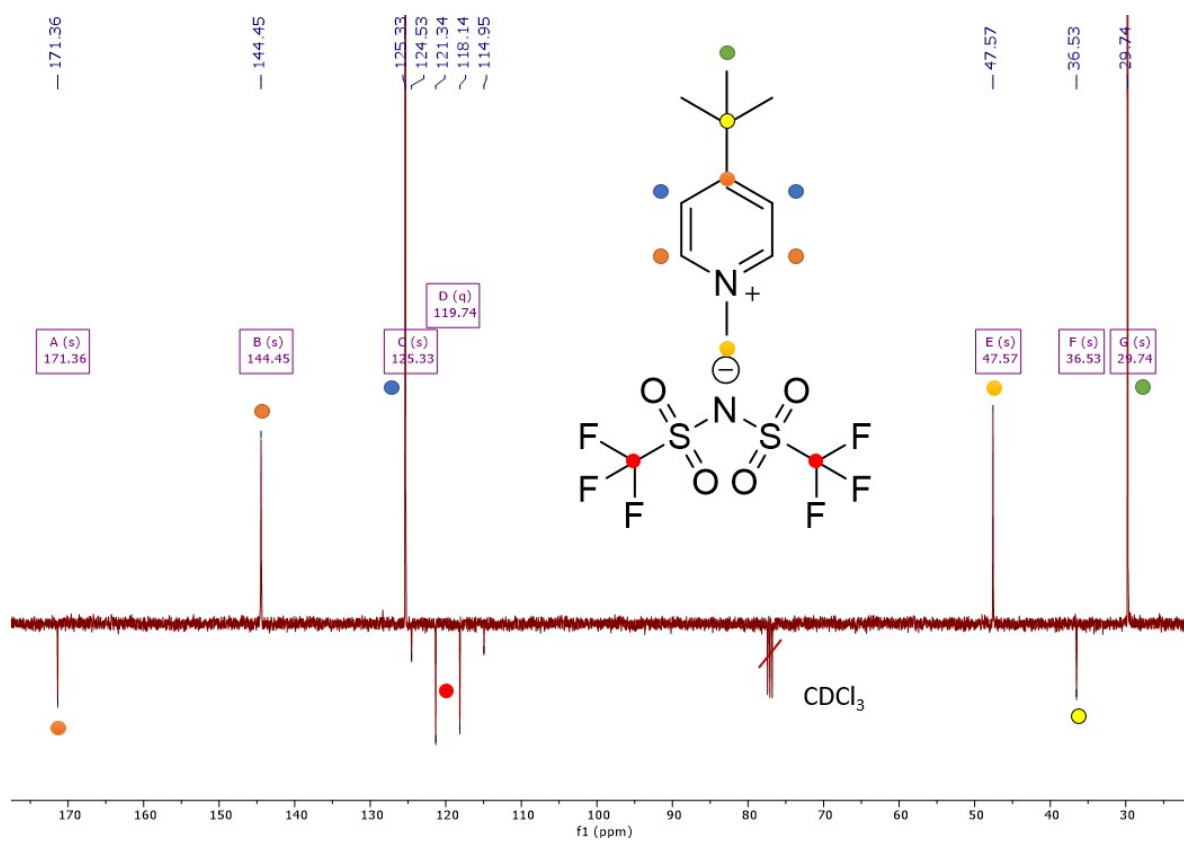


Figure S5. ^{13}C NMR APT spectrum of **IL** in CDCl_3

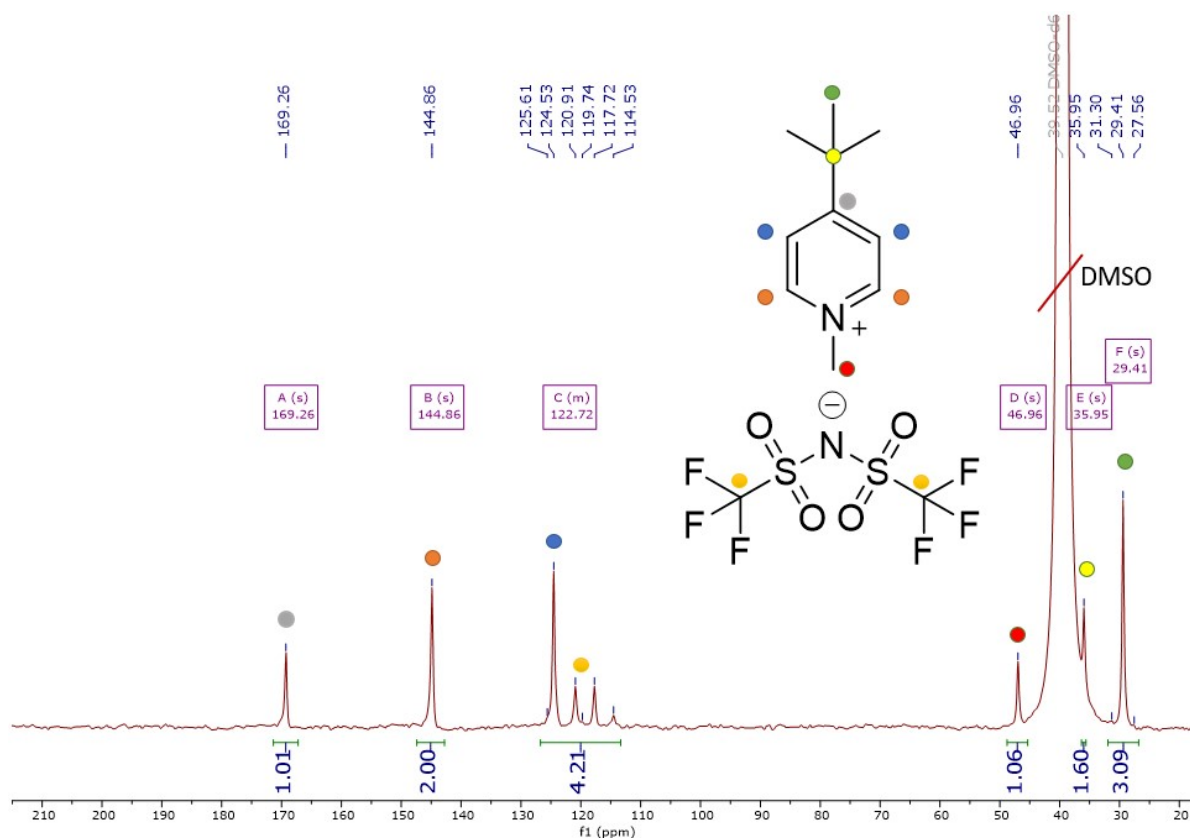


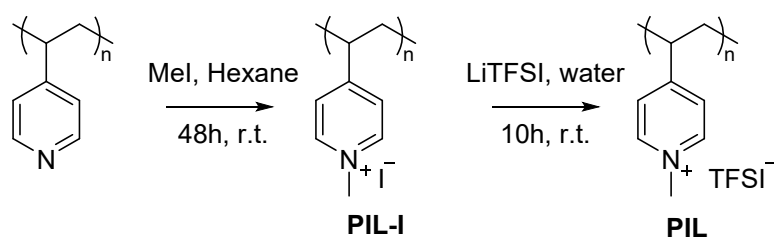
Figure S6. ¹³C NMR IG quantitative spectrum of **IL** in DMSO-d₆

4-(tert-butyl)-1-methylpyridinium tetrafluoroborate IL-BF₄

In a 50 mL beaker equipped with a magnetic stirrer, 0.5g (1.8 mmol) of 4-(tert-butyl)-1-methylpyridinium iodide (IL-I) was dissolved in 20 mL of DI water. An excess of four time of KBF₄ 0.91 g (7.2 mmol) was added to this solution. The solution immediately turned turbid and the mixture was stirred for 5 more hours in order to ensure the completion and then it was filtered. The white precipitate was washed three times with 20 mL water and dried under vacuum for 24 h. Yield 0.43 g (ca. 100%); m.p. 261-268 °C, FT-IR ν max [cm⁻¹]: 3073 =C-H, 2235 C≡N, 1612 -C=C-, 1408 -CH₂- scissoring, 1170 F-B-F asym. str., 1102 -SO₂-, 950 aromatic bending, 933 BF₄ asym. str., 655 bending =C-H.

¹H NMR (400 MHz, CDCl₃) δ 8.15 (d, J = 7.0 Hz, 2H), 7.47 (d, J = 7.0 Hz, 2H), 3.87 (s, 3H), 0.95 (d, J = 1.4 Hz, 9H). ¹³C NMR (101 MHz, CDCl₃) δ 171.42, 144.81, 125.36, 47.21, 36.08, 29.73. ¹⁹F NMR (377 MHz, DMSO-d₆) δ -148.17

3. PIL Synthesis and NMR data



Scheme S2. Synthetic route of PIL-I and PIL

Poly(4-vinyl-1-methylpyridinium iodide) PIL-I

The same procedure with the same molar equivalents has been applied in this case, elongating the time to allow all the polymer to react. Yield 1.34 g (67%); FT-IR ν max [cm⁻¹]: 3063 =C-H, 2249 C≡N, 1618 -C=C-, 1413 -CH₂- scissoring, 954 aromatic bending, 658 oop bending =C-H.

¹H NMR (400 MHz, DMSO-d₆) δ 8.64 (bs, 2H), 7.28 (bs, 2H), 4.22 (bs, 3H), 1.70 (bs, 3H).

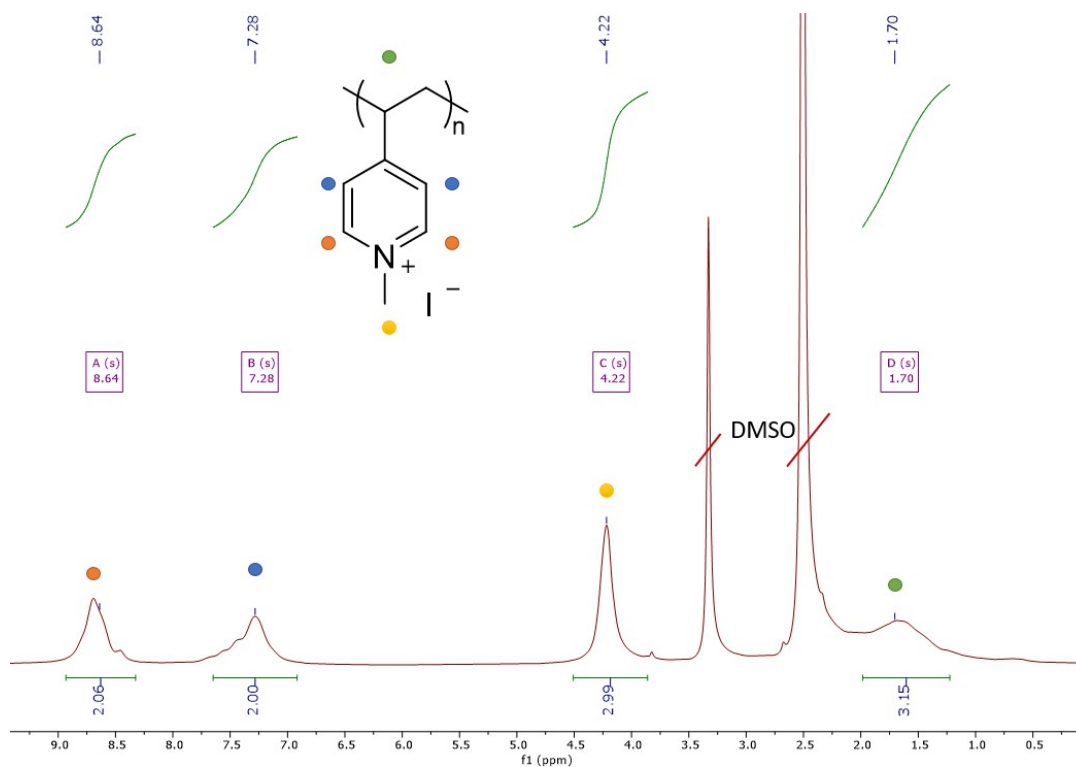


Figure S7. ¹H NMR spectrum of PIL-I in DMSO-d₆

Poly(4-vinyl-1-methyl-pyridinium iodide) PIL

The same procedure with the same molar equivalents has been applied in this case, elongating the time to allow all the polymer to react. Yield 0.55 g (72%); FT-IR ν max [cm⁻¹]: 3063 =C-H, 2250 C≡N, 1620 -C=C-, 1425 -CH₂- scissoring, 1267 -CF₃, 1105 -SO₂-, 996 aromatic bending, 780 scissoring CF₃, 645 oop bending =C-H.

¹H NMR (400 MHz, DMSO-d₆) δ 8.74 (bs, 2H), 7.95 (bs, 2H), 4.29 (bs, 3H), 1.90 (bs, 3H).

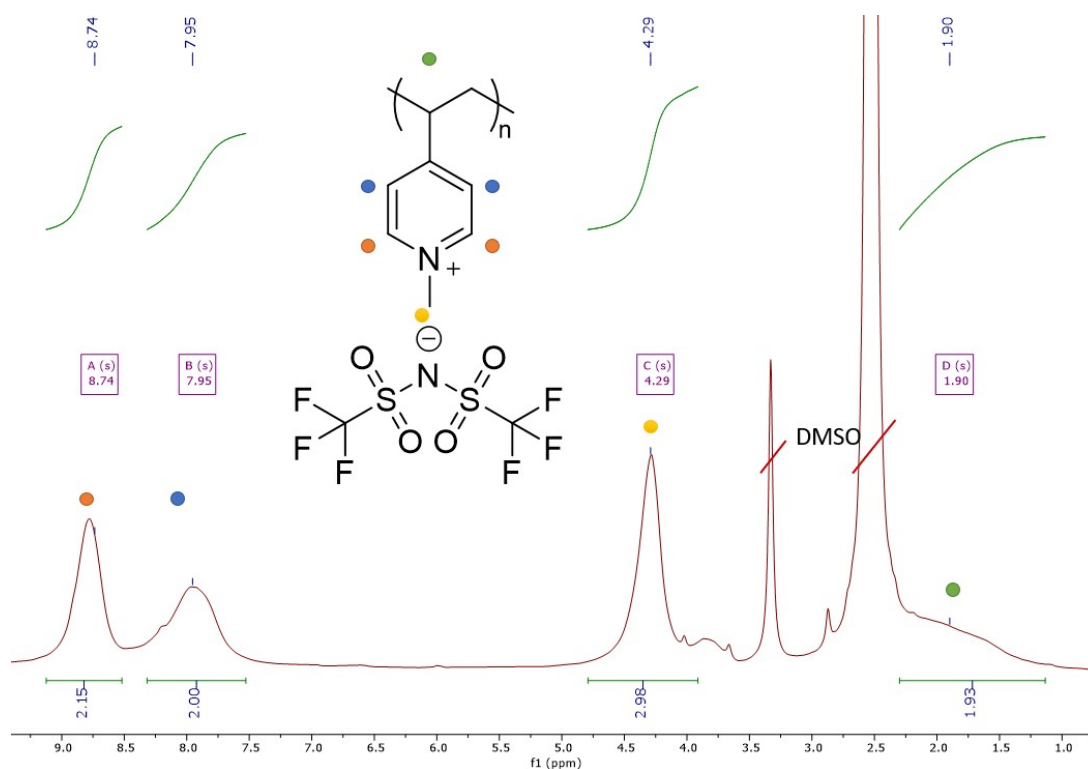


Figure S8. ¹H NMR spectrum of PIL in DMSO-d₆

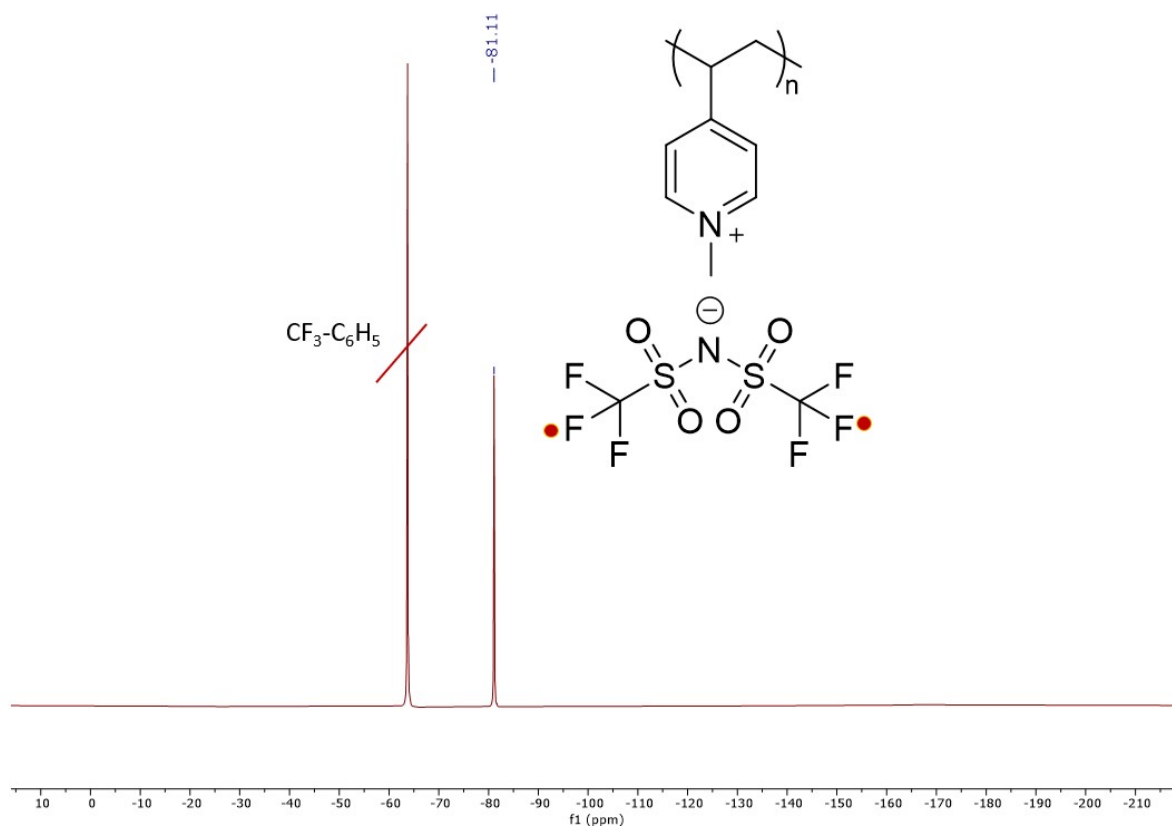


Figure S9. ^{19}F NMR spectrum of PIL in DMSO- d_6

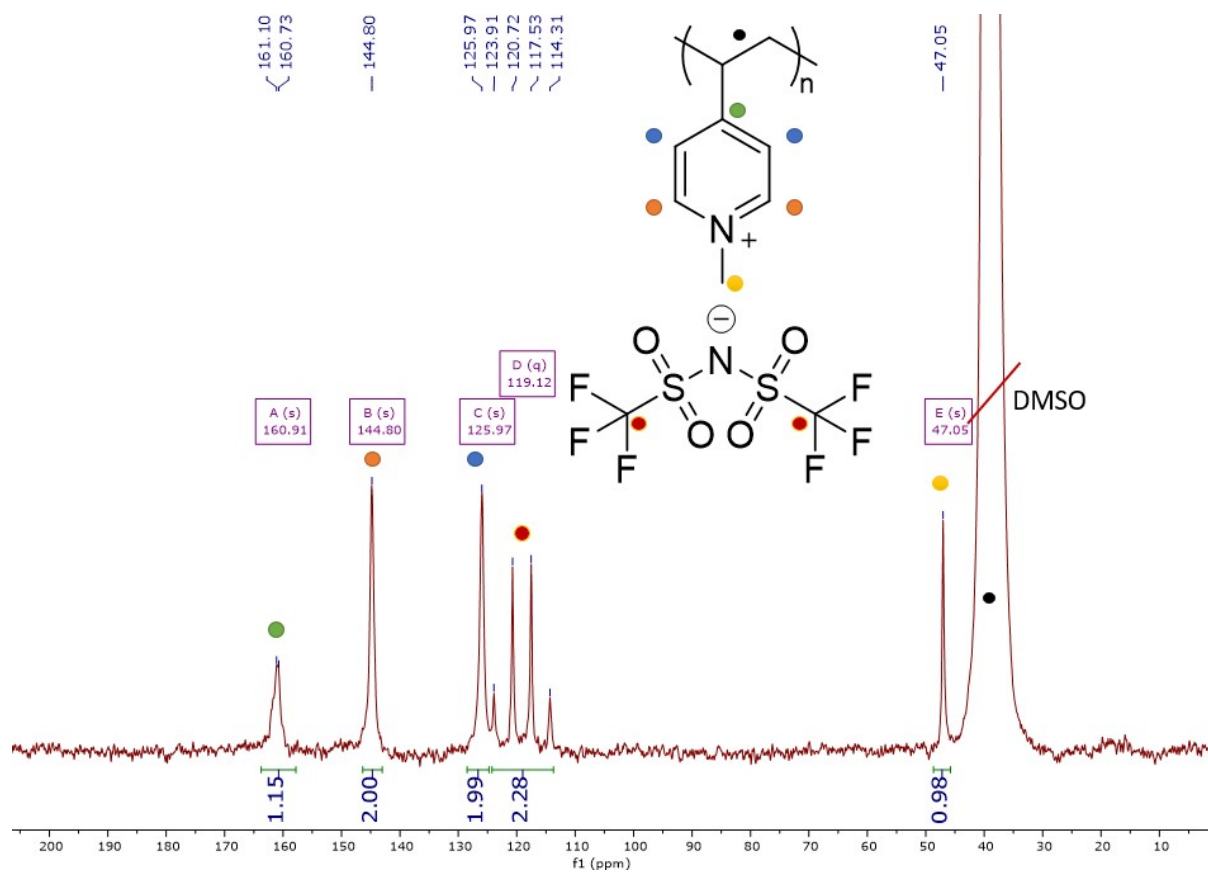


Figure S10. ^{13}C NMR IG quantitative spectrum of PIL in DMSO- d_6

Poly(4-vinyl-1-methyl-pyridinium iodide) PIL-BF₄

The same procedure with the same molar equivalents has been applied in this case, elongating the time to allow all the **PIL-I** to react. Yield 0.33 g (78%); FT-IR ν max [cm⁻¹]: 3073 =C-H, 2235 C≡N, 1612 -C=C-, 1408 -CH₂- scissoring, 1170 F-B-F asym. str., 1102 -SO₂-, 950 aromatic bending, 933 BF₄ asym. str., 655 bending =C-H.

¹H NMR (400 MHz, DMSO-d₆) δ 8.77 (bs, 2H), 7.91 (bs, 2H), 4.33 (bs, 3H), 1.79 (bs, 3H). ¹⁹F NMR (377 MHz, DMSO-d₆) δ -147.53.

4. Solar cell preparation

FTO glass with a sheet resistance of ~10 ohm/square from Nippon Sheet Glass Co. Ltd. was employed as a transparent conductive substrate. A series of cleanings using deionised water, acetone, ethanol, and UV-O₃ was conducted sequentially. Li-TFSI and Mg(TFSI)₂ were mixed in titanium diisopropoxide bis(acetylacetonate) as a precursor solution for the titania compact layer. A 40-nm-thick compact layer with a composition of Ti_{0.94}Li_{0.03}Mg_{0.03}O₂ was then prepared by the spray pyrolysis method at 550 °C. A mesoporous TiO₂ layer with a thickness of around 150 nm was then fabricated by spin coating with a TiO₂ (PST-24NR)-based solution. A perovskite precursor solution containing 1.5 M PbI₂, 1.25 M FAI, and 0.14 M CsI was prepared by dissolving all of the powders in DMF and DMSO mixed solvents with a volume ratio of 4:1. tBMPy-TFSI and PVMPy-TFSI additives were added to the precursor solution at different concentrations: 0.1, 0.15, 0.3 and 0.6% mol. A KI precursor solution with a molar concentration of 1.5 M was prepared separately, and added to be 2.5mol% into the above base precursor solution. Perovskite absorber layers were deposited using a spin-coating method (rotation speed: 4000 rpm for 10 s and 6000 rpm for 30 s) with anti-solvent treatment (500 μ L chlorobenzene quickly dropped 8 s prior to the end of the program). The hole transport material was then spin coated using 2,2',7,7'-Tetrakis[N,N-di(4-methoxyphenyl)amino]-9,9'-spirobifluorene (Spiro-OMeTAD) solution with a concentration of 54.2 mg/ml in chlorobenzene. Bis(trifluoromethane)sulfonimide lithium salt (Li-TFSI) (520 mg/mL in acetonitrile, 17.5 μ L) and tert-butyl pyridine tBP (32 μ L) were added to increase the conductivity. At last, Au (~100 nm) back contact was deposited by thermal evaporation with a contact area of 5.6 mm diameter and masked with an irradiation area of 0.18 cm². All processes were performed in a dry room (dewpoint temperature: -30 °C, room temperature from 21 to 25 °C. The corresponding RH for these conditions is 2.1% to 1.6%).

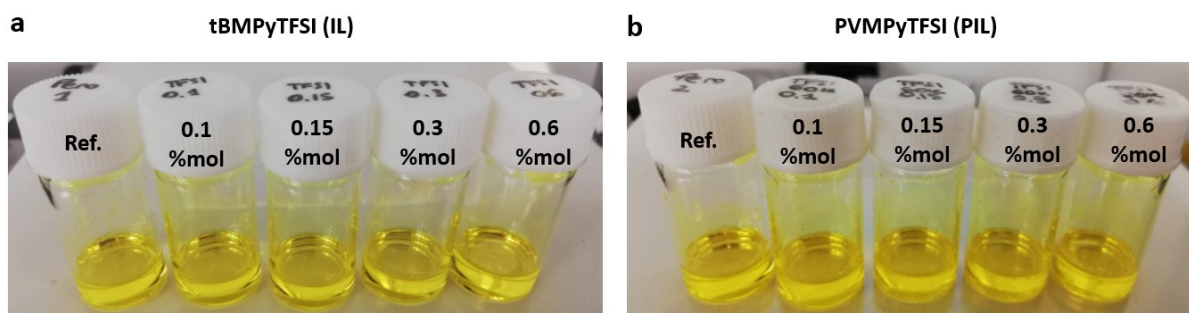


Figure S11. Perovskite precursor solutions with tBMPyTFSI (a) and PVMPyTFSI (b). In both pictures, a comparison with “Ref” (no additive) solution is presented. For tBMPyTFSI all solutions look very limpid, whereas solutions with PVMPyTFSI appear slightly turbid: the higher the PIL concentration and the more turbid the solution becomes.

5. Solar cell characterisation

XRD characterisation was conducted on a Bruker D8 Discover diffractometer with Cu K-alpha radiation ($\lambda = 0.15406$ nm). Transmittance and absorbance were measured with a spectrophotometer (UV3600, Shimadzu). SEM images were taken with a scanning electron microscope (Jeol 7800 -E Prime). The current density-voltage (J - V) curves were recorded under AM 1.5 G illumination (100 mW/cm²) with a 450-W xenon light source (YSS-80A; Yamashita Denso Co., Ltd., Japan). The scan speed was 200 mV/s and the calibration of the light source was performed using a Si photodiode of BS-520 (Bunkoukeiki Co., Ltd., Japan).

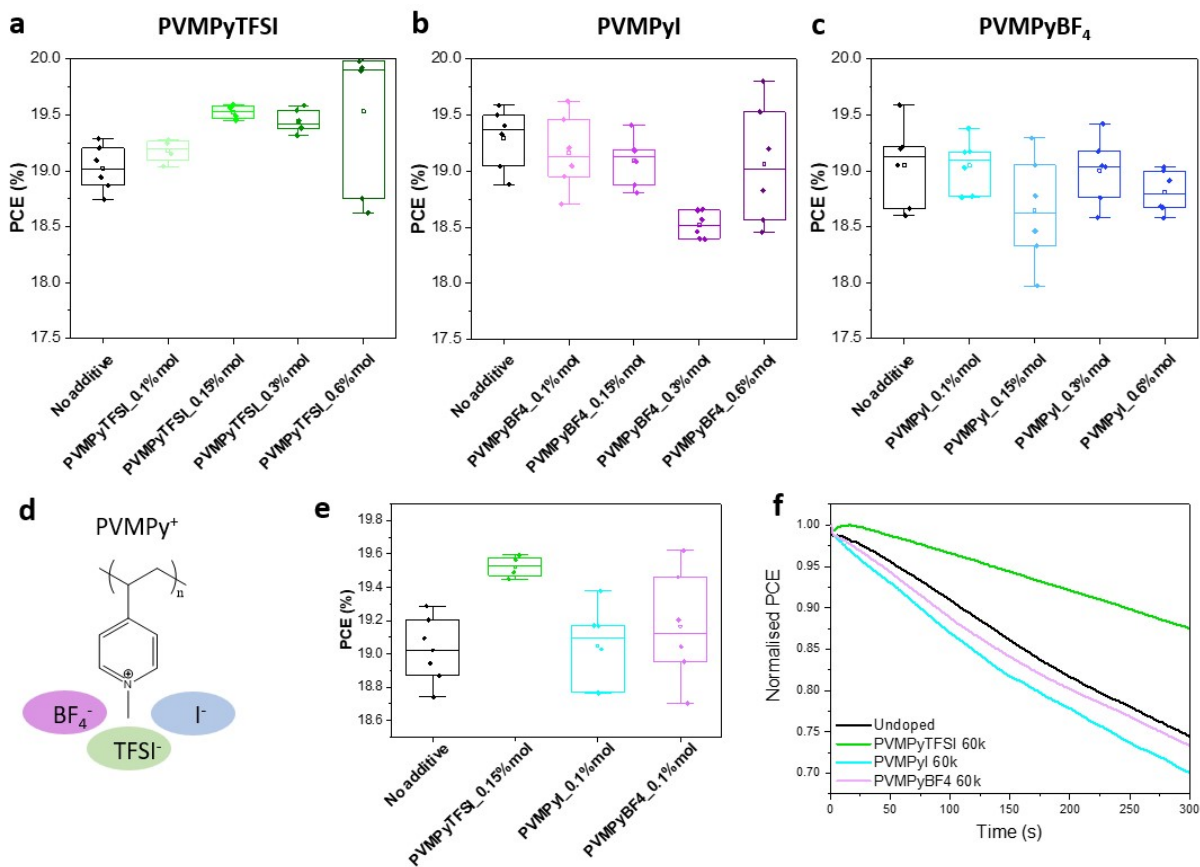


Figure S12. Comparison of device performance using PILs (60k g/mol) with different anions: TFSI⁻, I⁻, BF₄⁻. a, b and c) show the concentration optimisation of each PIL. d) Presents the PIL molecule with the three possible anions. e-f) show the direct comparison between PILs with different anions using the optimised concentration (TFSI⁻ = 0.15 %mol, I⁻ = 0.1 %mol, BF₄⁻ = 0.1 %mol), presenting both PCE (e) and MPP (f). Higher device PCE is obtained with TFSI⁻ counter anion together with a more stable MPP tracking over 5 minutes under AM1.5G illumination.

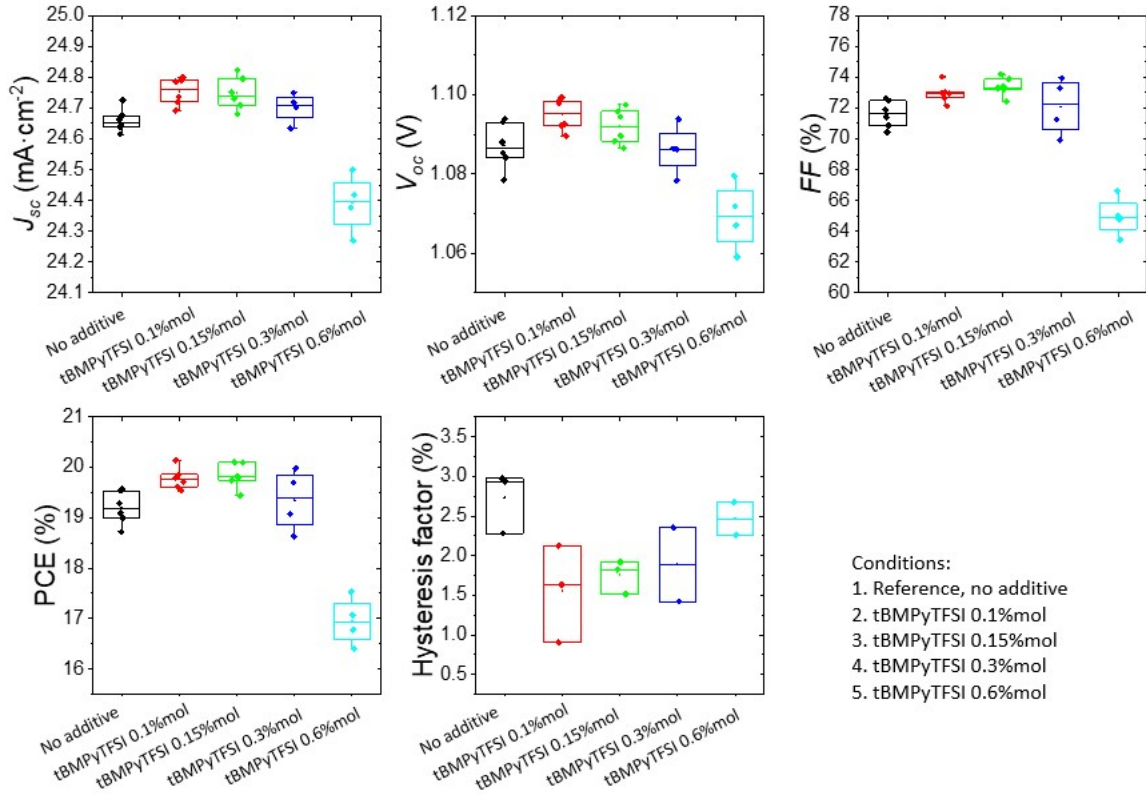


Figure S13. J-V parameters (J_{sc} , V_{oc} , FF, PCE and Hysteresis factor) of perovskite devices fabricated with tBMPy-TFSI. Concentrations between 0.1%mol and 0.6%mol were used to check the best device performances. J-V parameters of perovskite with IL were compared with “no additive” perovskite (neat) as reference.

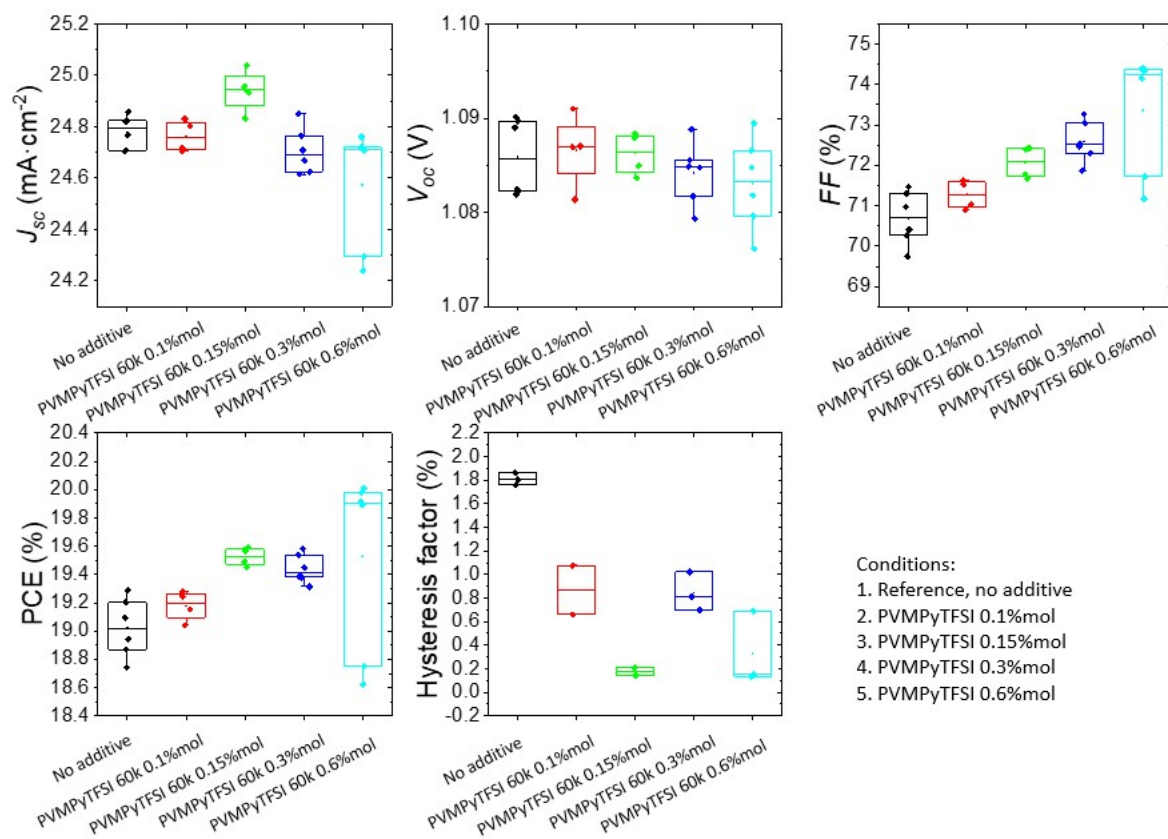


Figure S14. J-V parameters (J_{sc} , V_{oc} , FF, PCE and Hysteresis factor) of perovskite devices fabricated with PVMPy-TFSI. Concentrations between 0.1%mol and 0.6%mol were used to check the best device performances. J-V parameters of perovskite with PIL were compared with “no additive” perovskite (neat) as reference.

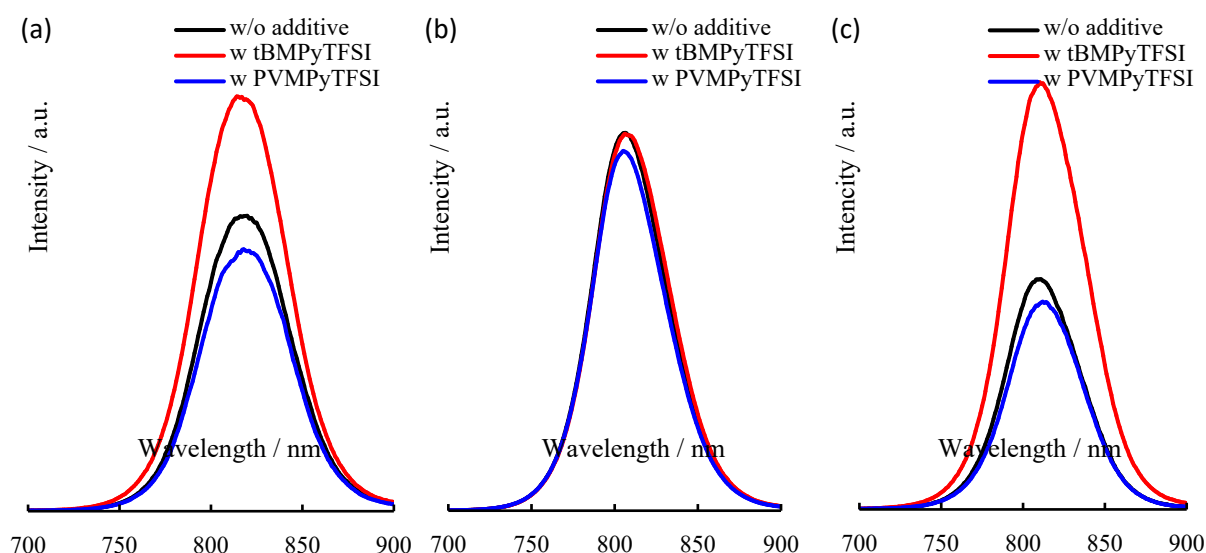


Figure S15. Steady state photo luminescence spectrum of Quartz/Perovskite (a), Quartz/TiO₂/perovskite (b), and Quartz/perovskite/Spiro-OMeTAD (c). Photoluminescence spectra were recorded with a charge-coupled detector cooled at -80°C with liquid N₂ using an excitation wavelength of $\lambda = 450$ nm from a Xe lamp as a light source in a spectrophotometer (JASCO FP-8700).

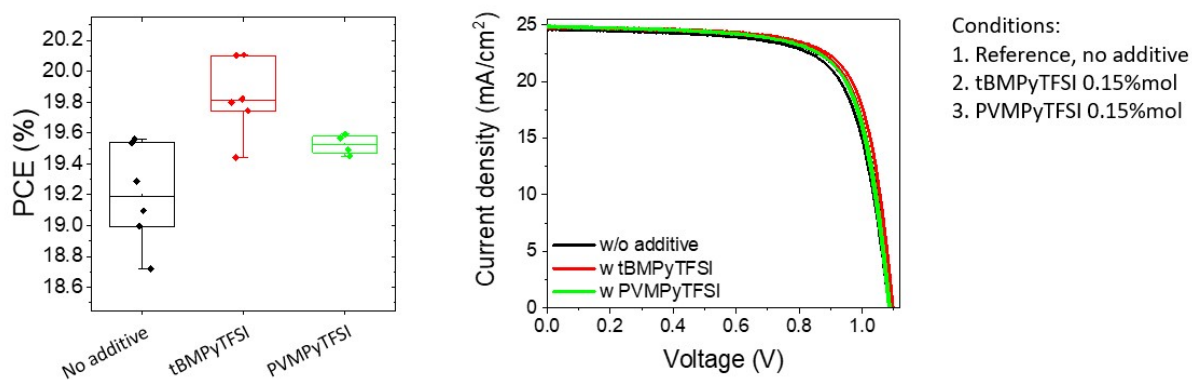
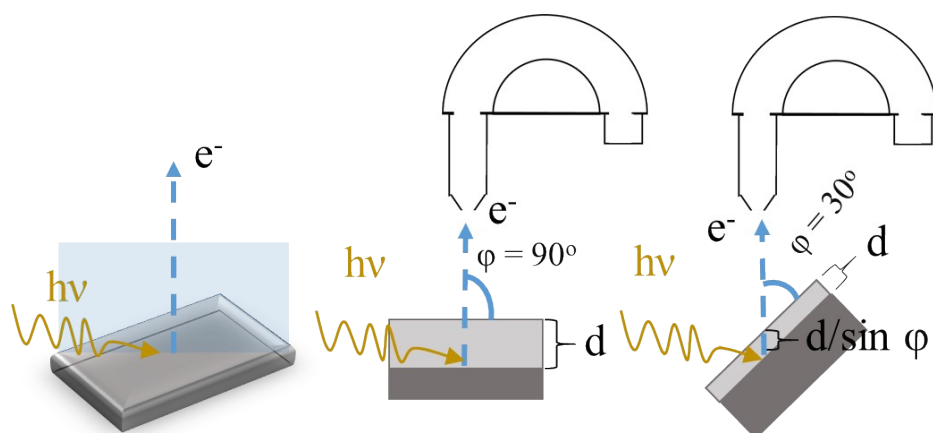


Figure S16. PCE statistics and JV curves of representative devices fabricated with undoped perovskite and containing 0.15%mol of tBMPy-TFSI (IL) and 0.15%mol PVMPy-TFSI (PIL).

Determination of surface stoichiometry from XPS investigations

Surface stoichiometry (Table S2) was determined from fresh perovskite films with or without



additives using to take-off angle as schematized in Fig. S13.

Fig S17: Schematic representation of the experimental set-up used to record XPS spectra using a conventional mode (take-off angle 90°) or a surface sensitive mode (take-off angle 30°).

Table S1: Binding energy values of the peaks detected on the X-ray photoelectron spectra using a conventional acquisition mode (take-off angle of 90°).

	C1s (eV)	N 1s (eV)	I 3d _{5/2} (eV)	I 4d _{5/2} (eV)	Pb 4f _{7/2} (eV)	Pb 5d _{5/2} (eV)	Cs 3d _{5/2} (eV)
without	288.5	400.9	619.5	49.5	138.7	19.8	725.2
with IL	288.5	400.8	619.5	49.5	138.6	19.8	725.2
with PIL	288.4	400.7	619.4	49.4	138.5	19.6	725.0

Table S2 : Experimental atomic ratios deduced from I 3d, F 1s, C 1s ($-\text{CF}_3$) and N 1s core level features recorded at different take-off angle for perovskite layers without additive, with tBMPy-TFSI or PVMPy-TFSI.

	Take-off angle	I / F	I / C (CF_3)	I / N
w/o additive	30°	-	-	2.6
	90°	-	-	2.1
tBMPy-TFSI	30°	3	4.1	2.1
	90°	6.6	9.2	2.0
	30°	3.8	5.9	2.0

PVMPy-TFSI	90°	6.6	5.5	1.7
------------	-----	-----	-----	-----

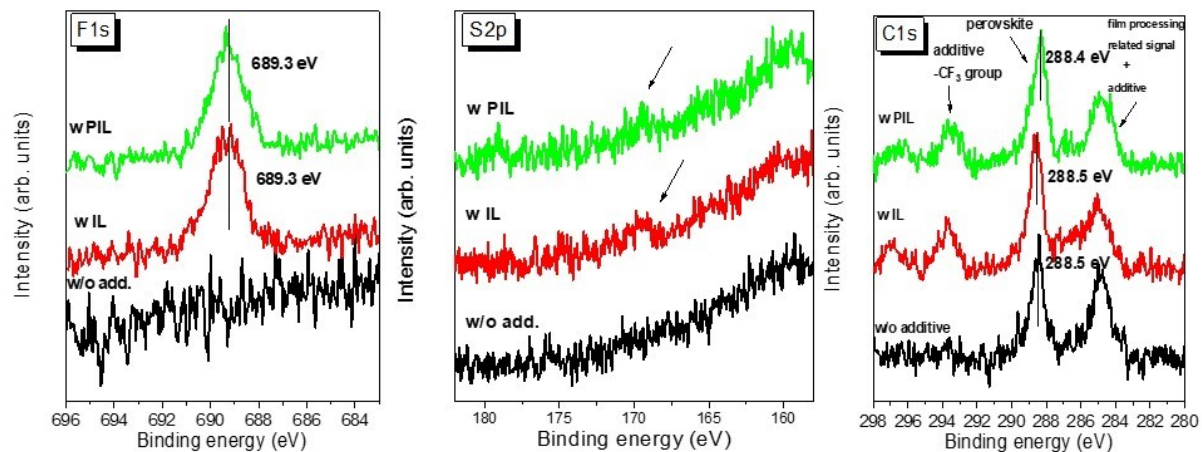


Fig. S18: XPS spectra for F 1s, S 2p and C 1s for perovskite layer without additive (black), with IL (red) and with PIL (green), recorded at a take-off angle of 90°. -CF₃ group is detected for both perovskite layers with IL and PIL additive, while it is absent for the neat perovskite layer.

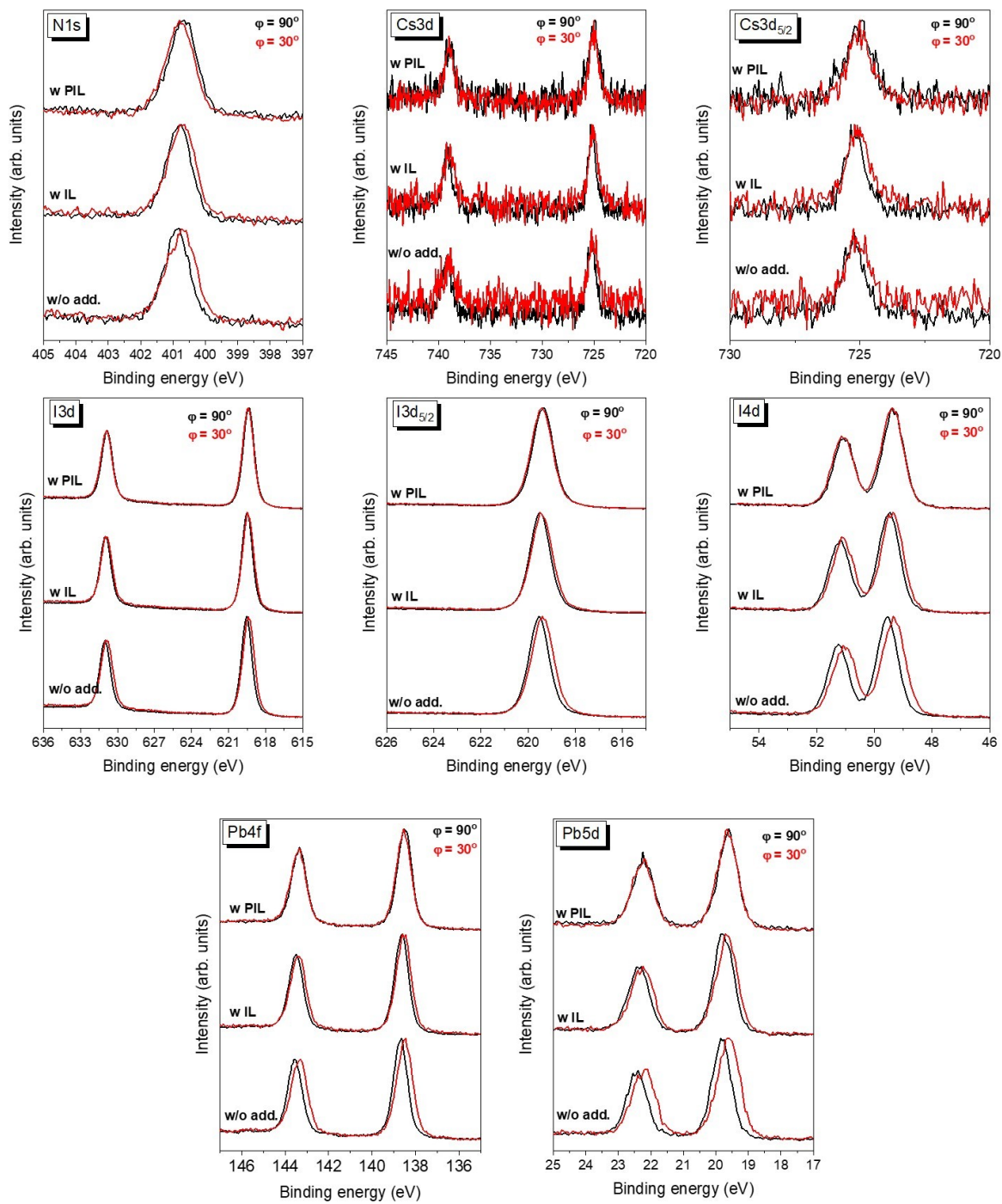


Fig. S19: XPS spectra for N1s, Cs 3d, I 3d, I 4d, Pb 4f and Pb 5d recorded at take-off angle of 90° (black) and 30° (red) for perovskite layer without additive, with IL and with PIL.

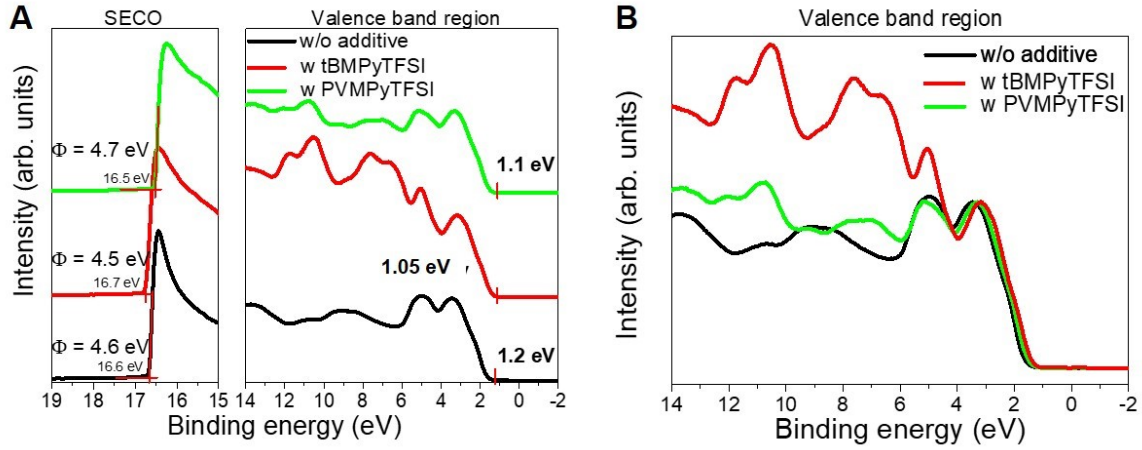


Fig. S20: UP spectra for perovskite layers without additive (black), with IL (red) and with PIL (green). A: Secondary Electron Cutoff and Valence Band regions; B: Normalized UP spectra in the Valence Band region.

Table S3: Electronic parameters deduced from UPS spectroscopy for the different layer present in the perovskite solar cell devices: Φ : Work Function; VBM (onset): Valence Band Maximum (onset); IP: Ionization Potential. Energy band gaps are also reported for sake of comparison. IL: tBMPy-TFSI; PIL: PVMPy-TFSI.

Film	Φ (eV)	VBM (eV)	IP (eV)	E_g (eV)
m-TiO ₂	3.6	3.5	7.1	-
Perovskite w/o additive	4.6	1.2	5.8	1.6 ^a
Perovskite with IL	4.5	≈ 1.05	5.55	1.6 ^a
Perovskite with PIL	4.7	1.1	5.8	1.6 ^a
Spiro-OMeTAD on perovskite	4.0	0.8	4.8	3.5 ^b
Spiro-OMeTAD on perovskite with IL	4.1	0.9	5.0	3.5 ^b
Spiro-OMeTAD on perovskite with PIL	4.1	0.8	4.9	3.5 ^b

^a Optical band gap determined in this study. ^b Value of the electronic band gap according to P. Schulz, E. Edri, S. Kirmayer, G. Hodes, D. Cahen and A. Kahn, *Energy Environ. Sci.*, 2014, **7**, 1377.

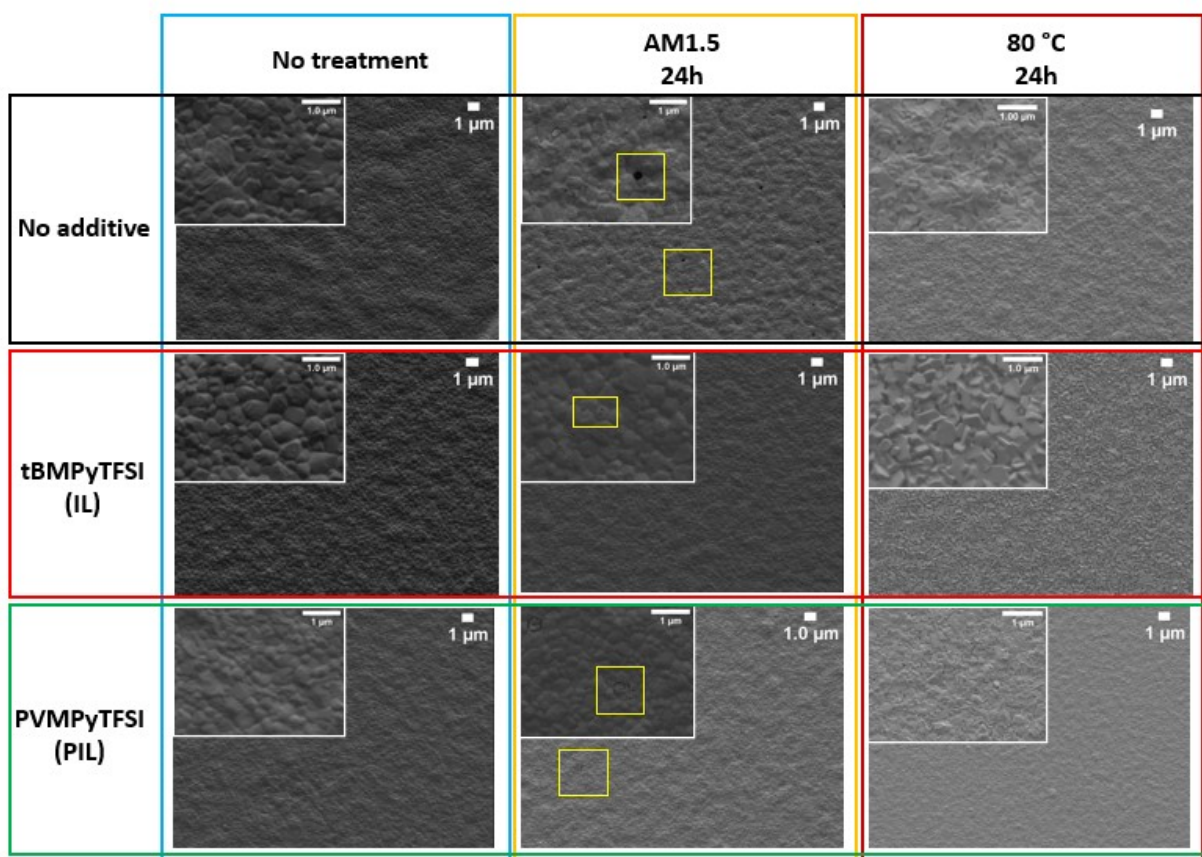


Figure S21. SEM images of the perovskite surface layer (pure, with IL and with PIL), deposited on glass/FTO/c-TiO₂/mp-TiO₂. Images compare fresh samples and samples that have been exposed to light (AM1.5) and heat (80 °C) for 24 hours in ambient conditions (*c.a.* 20 °C and 50% RH). Heat treatment was performed by putting samples on a hotplate and covered to avoid light exposure.

AM1.5 direct light exposure produces significant pin-holes in the additive-free perovskite layer, whereas for IL and PIL perovskite layers, pin-holes are present with much smaller dimensions.

Heat exposure on the contrary, shows a significant change of the crystal structure. In the case of additive-free perovskite and PIL/perovskite, the grains lose their grain density, as the grain “melt” with each other. On the contrary, in the case of IL/perovskite, perovskite grains become highly oriented.

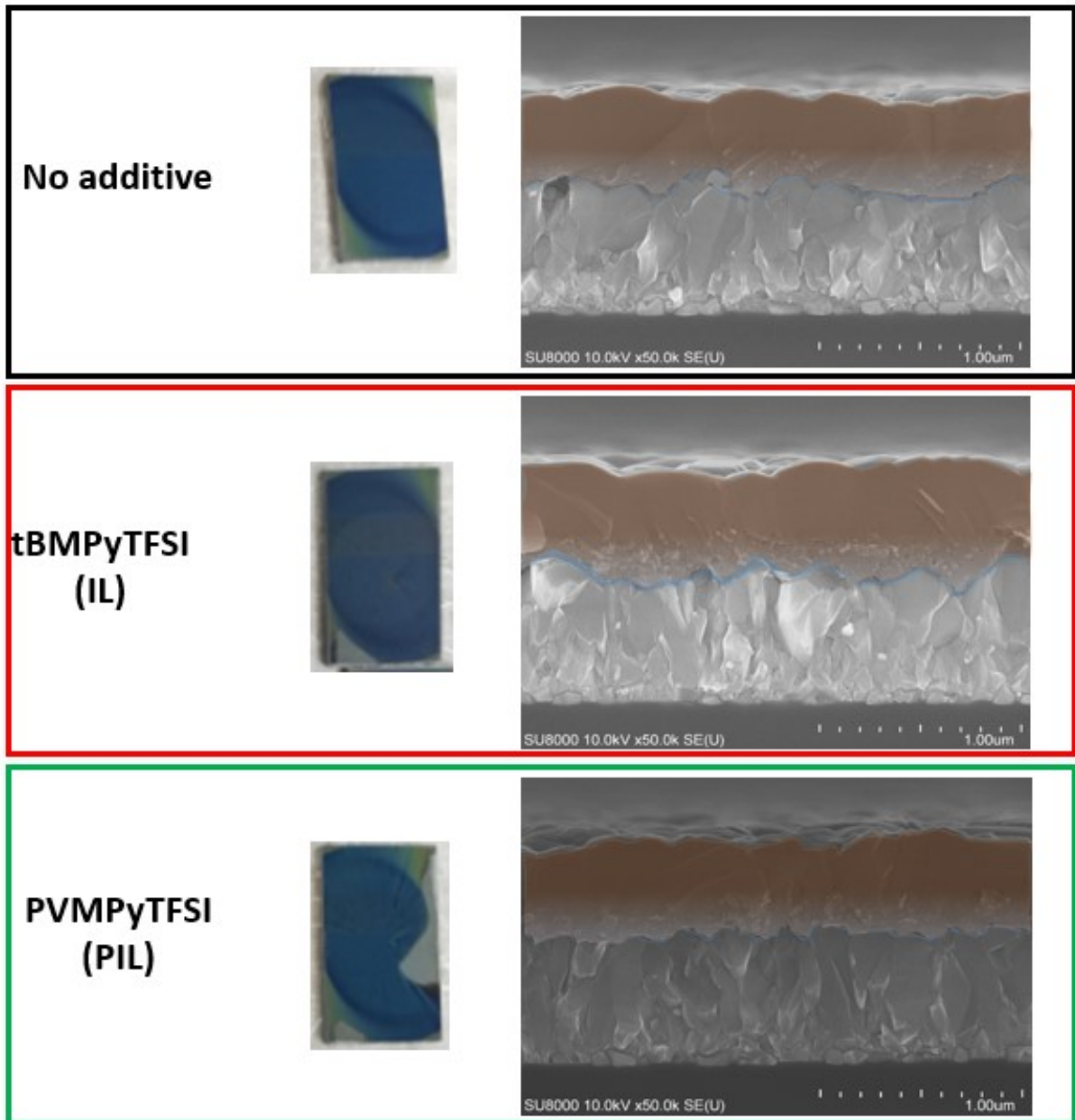


Figure S22. Film aspect of undoped perovskite and perovskite with tBMPy-TFSI and PVMPy-TFSI additive. Photographs present the devices just after spiro-OMeTAD spin-coating (missing only the Au back contact), showing that for IL and PIL/perovskites the wettability is lower compared to that of the perovskite without additive: for this reason, the perovskite films, and in particular the perovskite with the PIL additive, are not completely covered with spiro-OMeTAD on the device edges. On the right side of the photographs, SEM cross section of perovskite layers on glass/FTO/c-TiO₂/mp-TiO₂ are presented (brown = perovskite layer with gradient fill towards light blue = mp- and c-TiO₂).